

## Corrugated quantum well infrared photodetectors for polarization detection

C. J. Chen,<sup>a)</sup> K. K. Choi,<sup>b)</sup> L. Rokhinson, W. H. Chang,<sup>b)</sup> and D. C. Tsui  
*Department of Electrical Engineering, Princeton University, Princeton, New Jersey 08544*

(Received 12 October 1998; accepted for publication 1 December 1998)

In this letter, we propose the use of the newly developed corrugated quantum well infrared photodetectors (C-QWIPs) for polarization detection. The corrugated structure, which serves as an optical coupler as well as the polarization-sensitive component, is in this case directly created into the active region of the QWIP, therefore dispensed with the need of an external polarizer. Moreover, four C-QWIPs with differently oriented corrugated patterns can be integrated as one unit, thus allowing a precise, real-time measurement of the polarization state. The polarimetry of this detector unit was characterized using a blackbody source and a metal grating polarizer. © 1999 American Institute of Physics. [S0003-6951(99)00706-8]

Over the past several years, the development of thermal imaging systems has been progressing rapidly. However, conventional infrared detectors, which detect the intensity of thermal radiation emitted and reflected from objects, are limited in their usefulness by the low contrasts in terrestrial scenes. On the other hand, the polarization of the thermal radiation in the same scenes often has high contrast, due to the differences found in the shape and optical properties between natural and artificial surfaces.<sup>1</sup> The use of infrared (IR) detectors, which can capture both polarization and intensity data, will lead to significant improvement in target recognition functions by providing enhanced spatial resolution of the target, the ability to suppress unpolarized background radiation, and the capability for zero  $\Delta T$  imaging. A polarization-sensitive imaging system would have immediate applications in several areas, including mine field detection, robotic vision, material classification, oceanography, and agriculture.

At the present time, the most commonly adopted method for polarization detection is to attach a rotating polarizer in front of the photodetectors. The polarization state of the incoming radiation is determined by serially rotating the polarizer and then recording the detector response at each polarizer orientation. There are inconveniences in using such a composite system. In addition to its clumsiness, it is sometimes not feasible to gather, in this serial way, complete information of a fast moving object. In this letter, we propose a new method utilizing the recently developed corrugated quantum well infrared photodetector (C-QWIP) technology to detect the polarization state of the incident radiation. The polarization-sensitive component of this system, i.e., the corrugated coupling structure, is directly fabricated into the detector active region, thus dispensed with the use of an external polarizer. Moreover in this system a set of four detectors, each sensitive to a different polarization direction, is grouped

as one unit which can simultaneously gather all polarization information to avoid the temporal variations of a fast changing signal. Such a system is therefore ideal for smaller and faster sensors that can be easily used in many circumstances.

In a QWIP structure, due to the dipole selection rule, only light with an electric field component perpendicular to the quantum well (QW) planes can be absorbed. As a result, the incorporation of an optical coupler is necessary to channel normal incident light into the favorable directions for infrared absorption. Among the existing coupling approaches, the use of C-QWIPs has been demonstrated to be simple and efficient in coupling the *s*-polarization component (i.e., the electric field perpendicular to the corrugated lines) of the incident radiation.<sup>2</sup> To completely characterize the polarization state of the incoming signal, four C-QWIPs with corrugated lines along  $90^\circ$  (device A),  $0^\circ$  (device B),  $\pm 45^\circ$  (devices C and D) orientations, as shown in Fig. 1(a), are required. In general, the intensity of the incoming radiation consists of the polarized part  $I_p$  and the unpolarized part  $I_u$ :

$$I = I_u + I_p = \left(\frac{1}{2}I_u + \frac{1}{2}I_u\right) + [I_p(0^\circ) + I_p(90^\circ)]. \quad (1)$$

The photocurrent of device A can be expressed as:

$$J_A = R_A(0^\circ) \times \left[\frac{1}{2}I_u + I_p(0^\circ)\right] + R_A(90^\circ) \times \left[\frac{1}{2}I_u + I_p(90^\circ)\right], \quad (2)$$

where  $R_A(0^\circ)$  and  $R_A(90^\circ)$  are the responsivities of device A for radiation polarized along  $\hat{x}$  and  $\hat{y}$ , respectively. Similar expressions can be written down for photocurrents of the other three devices. After some rearranging, we get:

<sup>a)</sup>Electronic mail: cjchen@ee.princeton.edu

<sup>b)</sup>Present address: US Army Research Laboratory, 2800 Powder Mill Rd., Adelphi, MD 20783.

$$\begin{pmatrix} I_u \\ I_p(0^\circ) \\ I_p(90^\circ) \end{pmatrix} = \begin{pmatrix} \frac{R_A(0^\circ) + R_A(90^\circ)}{2} & R_A(0^\circ) & R_A(90^\circ) \\ \frac{R_B(0^\circ) + R_B(90^\circ)}{2} & R_B(0^\circ) & R_B(90^\circ) \\ \frac{R_C(45^\circ) + R_D(45^\circ)}{2} & \frac{R_C(45^\circ) + R_D(45^\circ)}{2} & \frac{R_C(45^\circ) + R_D(45^\circ)}{2} \end{pmatrix}^{-1} \begin{pmatrix} J_A \\ J_B \\ \frac{J_C + J_D}{2} \end{pmatrix} \quad (3)$$

with various  $R_s$  as the corresponding responsivities of the four devices. The angle  $\theta$  of the polarized component of the incident radiation, measured from  $\hat{x}$  in Fig. 1(a), is:

$$\theta = \frac{J_D - J_C}{|J_D - J_C|} \cdot \tan^{-1} \left( \sqrt{\frac{I_p(90^\circ)}{I_p(0^\circ)}} \right). \quad (4)$$

With pre-calibrated  $R_s$ , the measured photocurrents of the four devices completely determine the polarization state of the incoming radiation.

The QWIP sample used in this work consists of a multiple quantum well (MQW) stack sandwiched between two 5000 Å GaAs contact layers. The MQW stack is made of 23 periods of 500 Å Al<sub>0.28</sub>Ga<sub>0.72</sub>As barriers and 50 Å GaAs wells. Its detection peak  $\lambda_p$  is designed to be around 9 μm. The doping density  $N_d$  is  $0.5 \times 10^{18} \text{ cm}^{-3}$  in the wells of the MQW stack, and  $1 \times 10^{18} \text{ cm}^{-3}$  in the contact layers. Four devices with corrugated lines oriented along different crystallographic directions have been fabricated. For the chemical solution used in this work (1H<sub>2</sub>SO<sub>4</sub>:8H<sub>2</sub>O<sub>2</sub>:8H<sub>2</sub>O), the etching rate is different for different crystallographic planes. Figures 1(b), 1(c), and 1(d) show the profiles of the four devices as viewed along the dashed lines in Fig. 1(a). Device A consists of an array of triangular prisms, of which the sidewalls can reflect the normal incident light into a nearly parallel direction. Device B has an undercut profile while the other two devices have vertical sidewalls with curved bottoms. These three devices utilize single slit diffraction to create favorable optical paths for infrared absorption. Since devices C and D have the same etching profiles, they show similar performance and we have  $R_C(45^\circ) = R_D(-45^\circ)$  and

$R_C(-45^\circ) = R_D(45^\circ)$ . We therefore present in this letter only the experimental data for devices A, B, and C.

The current–voltage ( $I$ – $V$ ) characteristics of devices A, B, and C are shown in Fig. 2, with  $J_d$  representing the 77 K dark current and  $J_p$  the 300 K background photocurrent measured at 10 K through a 36° field of view. It is clear from Fig. 1 that more detector active materials are removed from devices B and C than from device A. As a result, the dark currents of devices B and C are lower than that of device A. There is a corresponding reduction in the background photocurrent for devices B and C as well. The inset of Fig. 2 shows the photocurrent to dark current ratio  $J_p/J_d$  for these three devices. Device B has a higher current ratio, indicating a better coupling efficiency compared to that of device A. Since the purpose of this work is to demonstrate the use of C-QWIPs as polarization detectors, the various corrugated patterns employed here are not optimized to provide the best coupling efficiency. Improved performance is expected for devices with properly designed patterns.

In order to obtain various  $R_s$  in Eq. (3), ac spectral photocurrent measurements were performed at 10 K with a rotating polarizer inserted between the monochromator and the C-QWIPs. As the monochromator itself partially polarizes the light, the power coming out of it is different for different polarization directions. We have calibrated the power using a HgCdTe detector. The spectral responsivities of devices A, B, and C, measured at an applied bias 2V with the polarizer oriented at 0°, 90°, and ±45°, are shown in Fig. 3. With  $R_s$  calibrated, the information obtained from the photocurrent measurement is then sufficient to determine the polarization state of the incoming signal.

As mentioned previously, C-QWIPs are more sensitive

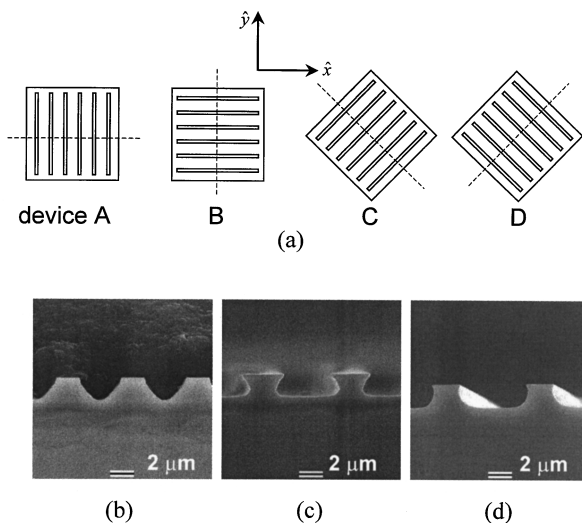


FIG. 1. Relative orientations of devices A, B, C, and D used in this work for polarization detection (a), and the scanning electron microscope (SEM) pictures showing the profiles of devices A (b), B (c), C and D (d), cut along the dashed lines in (a).

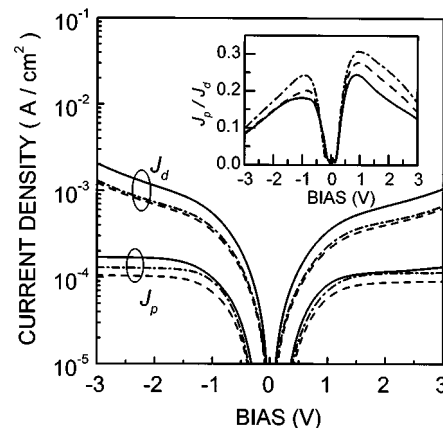


FIG. 2. The  $I$ – $V$  characteristics of devices A (solid curves), B (dash-dot curves), and C (dashed curves), with  $J_d$  the 77 K dark current, and  $J_p$  the 300 K background photocurrent. Inset shows the photocurrent to dark current ratios for these three devices.

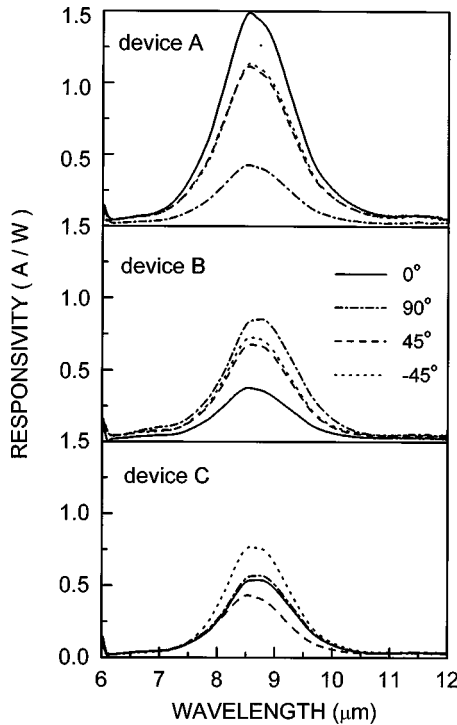


FIG. 3. The responsivities of devices A, B, and C, with the transmission axis of the polarizer oriented at four different angles:  $0^\circ$  (solid curves),  $90^\circ$  (dash-dot curves),  $+45^\circ$  (dashed curves), and  $-45^\circ$  (dotted curves).

to the  $s$ -polarized light (perpendicular  $E$  field) than to the  $p$ -polarized light (parallel  $E$  field). For further characterization on the polarimetry of the C-QWIPs, photocurrents of the four devices were measured as functions of the polarizer orientation, using a blackbody radiator as the light source. Figure 4 shows the angular dependence of the photocurrents for devices A, B, and C, with  $\theta$  the angle between the transmission axis of the polarizer and  $\hat{x}$ . The polarization sensitivity of these devices is clear. For linearly polarized light,  $I(0^\circ) = I \cos^2 \theta$  and  $I(90^\circ) = I \sin^2 \theta$ . The photocurrent of device A can be written as:

$$J_A = \frac{1}{2} \{ [R_A(0^\circ) + R_A(90^\circ)] + [R_A(0^\circ) - R_A(90^\circ)] \cos 2\theta \}. \quad (5)$$

From data fitting (dashed curve in Fig. 4), we get  $J_A = 6.6 + 3.3 \cos 2(\theta - 5.8^\circ)$  in arbitrary unit, or  $R_A(0^\circ) = 3R_A(90^\circ)$ , consistent with the result of spectral measurements (Fig. 3). The phase  $5.8^\circ$  accounts for the misalignment between the detectors and the polarizer. Similarly,  $R_B(90^\circ) = 2R_B(0^\circ)$  and  $R_C(-45^\circ) = 1.7R_C(45^\circ)$ .

Although four detectors are required for a complete characterization of the polarization state, such detailed information is generally not necessary to achieve the object of distinguishing an entity from its unpolarized background. Any physical quantity containing the polarization information may be sufficient for this purpose. To simplify the fabrication procedure as well as increase the resolution of a camera array, we propose using the photocurrent ratio ( $r$ ) between two detectors, namely A and B, as the polarization-sensitive parameter. It is evident from Eq. (2) that  $r$  depends on the degree of polarization, as well as the angle  $\theta$ . The value of  $r$  could be different for signals with different polarization states and, therefore, is a useful parameter when the object to be detected from a scene with low thermal contrast

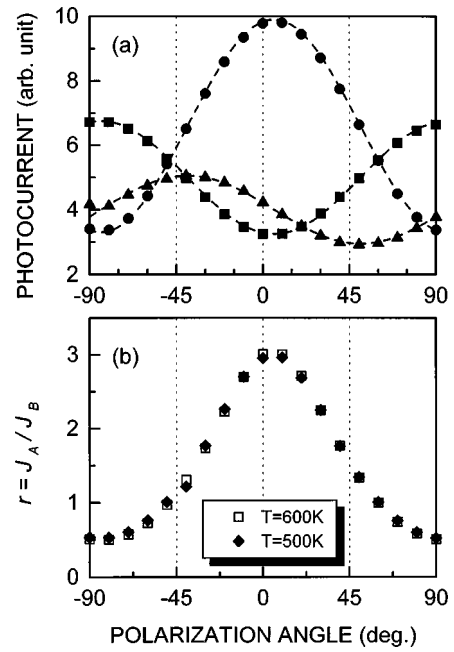


FIG. 4. (a) Photocurrents of devices A (solid circles), B (solid squares), and C (solid triangles) as functions of the polarizer orientation. The dashed curves are fits using Eq. (5). (b) The current ratio of devices A and B with the blackbody source set at two different temperatures 600 K (open squares) and 500 K (solid diamonds).

has a high degree of polarization.

As a demonstration, we again used linearly polarized light and then measured the photocurrent ratio of devices A and B. From Eq. (5):

$$\frac{J_A}{J_B} = \frac{[R_A(0^\circ) + R_A(90^\circ)] + [R_A(0^\circ) - R_A(90^\circ)] \cos 2\theta}{[R_B(0^\circ) + R_B(90^\circ)] + [R_B(0^\circ) - R_B(90^\circ)] \cos 2\theta}. \quad (6)$$

The dependence on light intensity cancels out, and the detection under this situation is completely independent of the radiation level of the object. This intensity independence has been experimentally verified by setting the blackbody source at two temperatures (600 and 500 K) and then comparing the respective current ratios [Fig. 4(b)]. Although the radiation intensities differ by two times, the current ratios remain the same within 5% error bar.

In conclusion, we have demonstrated the use of C-QWIPs for infrared polarization detection. In this structure, the polarization-sensitive components are directly integrated into the photodetectors and they allow the collection of all polarization information in one single video frame if necessary. The device is simple and fast, therefore ideal for applications where compactness of the measurement system or the ability to capture fast changing images is of great importance.

The authors would like to thank Steve Chou and D. W. Beekman for useful conversations. The work at Princeton University was supported by a grant from the ARO.

<sup>1</sup> C. S. L. Chun, D. L. Fleming, W. A. Harvey, and E. J. Torok, Proc. SPIE **2552**, 438 (1995); M. A. LeCompte, F. J. Iannarilli, D. B. Nichols, and R. K. Keever, Proc. SPIE **2496**, 180 (1995).

<sup>2</sup> C. J. Chen, K. K. Choi, M. Z. Tidrow, and D. C. Tsui, Appl. Phys. Lett. **68**, 1446 (1996); C. J. Chen, K. K. Choi, W. H. Chang, and D. C. Tsui, Appl. Phys. Lett. **71**, 3045 (1997); C. J. Chen, K. K. Choi, W. H. Chang, and D. C. Tsui, IEEE Trans. Electron Devices **45**, 1432 (1998).